EPJ Web of Conferences **371**, 01013 (2026) https://doi.org/10.1051/epjconf/202637101013
AMT'2026

Effect of the magnetic field on the heat transfer enhancement of nanofluids in rectangular enclosures

Bilal El hadoui[1*], *Youness* Ighris[2], *Mohamed* Rahmoun[3], *Mourad* Kaddiri[4], and *Jamal* Baliti[2]

[1]Rabat National School of Mines (ENSMR), BP: 753 Agdal-Rabat, Morocco
[2]Research team in Smart Electrical, Mechanical and Energy Systems (SEMES), Polydisciplinary Faculty, University of Sultan Moulay Slimane, Beni Mellal, Morrocco
[3]Multidisciplinary Research Laboratory in Physics (M.R.L.P), Polydisciplinary Faculty, Sultan Moulay Slimane University, Beni Mellal, Morocco
[4]Laboratory of Intelligent Systems, Advanced Mechanics and Renewable Energy, Faculty of Sciences and Technologies, Sultan Moulay Slimane University, Beni-Mellal, Morocco

Abstract. The application of a magnetic field tends to reduce the convective flows in enclosures, thereby decreasing convective heat transfer. However, adding nanoparticles to the fluid improves both thermal conductivity and viscosity, thus improving the conductive heat transfer. The enhanced total heat transfer is desirable in engineering problems like cooling systems for electronic devices. Therefore, the research for the best control of the pertinent parameters is a must. In this study, nanofluid convective heat transfer is investigated, seeking the best control of the governing parameters, namely, the Hartmann number $0 \leq Ha \leq 80$, aspect ratio $0.25 \leq A \leq 4$, and Al_2O_3 nanoparticle volume fraction $0 \leq \varphi \leq 0.05$. Results show that the relationship between the heat transfer and nanoparticle volume fraction is different depending on A and Ha. In the absence of a magnetic field, there exists a critical value of A beyond which this relationship changes from enhancing to deteriorating heat transfer, whereas the application of a magnetic field leads to enhanced heat transfer with the use of nanofluids in horizontal enclosures which is due to the weakening effect on the flow that the magnetic field plays and leads to a strengthening effect of the nanofluid thermal conductivity over viscosity.

1 Introduction

Natural convection in enclosures remains a broad field with extensive engineering applications. Examples of such applications include solar energy harvesters, heat insulation for buildings, cooling designs for electronic components, and designs for nuclear reactors. In such scenarios, buoyancy-induced flows determine heat transfer phenomena and become a critical factor for optimal design and efficient operation of thermal systems. Additionally, apart from such conventional setups, recent experimental and numerical studies continue to

* Corresponding author: bilal.elhadoui@usms.ac.ma

expand our scope of naturally buoyancy-induced convection phenomena in complex geometries and boundary conditions. For example, Wang et al. [1] performed an experimental study of natural convection in a V-cavity with a lower heating surface and upper cooling surface. They reported the time-dependent evolution of a conduction-dominated to fully developed convection flow process. Chen et al. [2], for instance, used a numerical model based on inverse natural convection with a horizontal metallic fin. They observed how a correct model for turbulent convection depends largely on geometric parameters for a horizontal metallic cavity with varying Rayleigh number. Following a similar track, a numerical and experimental study by Weppe et al. [3] analysed turbulent natural convection with a partly heated internal obstacle in a cubic cavity. They identified a recirculated region hampering heat stratification. For accentuating complexities inherent with buoyancy-induced convection in enclosures, there are studies such as those conducted by Yoladi et al. [4]. They identified inclination effects leading to differing buoyancy-induced melting designs for phase-change-material designs. Several comprehensive review articles have summarized the fundamental mechanisms, flow regimes, and geometric influences governing natural convection in enclosures that one can look at [5].

In some practical applications, such as crystal growth in fluids, the presence of a magnetic field complicates this process of convection. The interaction between the magnetic field and the electrically conducting fluids in the enclosure generates a Lorentz force that changes the flow behaviour and heat transfer characteristics. The interaction has been widely noticed because it opens avenues for a large number of applications in high-technology and industrial applications related to the control and optimization of thermal management systems. A profound examination of natural convection with a multi-directional external magnetic field in a square cavity with sinusoidal wall heating and internal heated and cooled obstacles was made by Hamid et al. [6]. It was concluded that an increase in almost all the parameters, except *Ha*, augments the heat transfer inside the enclosure. A similar examination was made on the inclined magnetic field effect within square cavities by Liao and Li [7]. Their results explained a modification in heat transfer transitions based on external magnetic fields. A recent contribution toward this examination was made by Mohammadi and Nassab [8]. This particular examination was made for elliptical internal heaters with a two-fold effect of an external magnetic field and radiation. Their results clearly revealed intensity modification up to a maximum of 66 % without radiation. Furthermore, Li et al. [9] considered the effect of an external magnetic field on momentum and heat transport in Rayleigh-Bénard convective flows within cavities containing electrically conductive molten salt. They showed that the magnetic field has a stabilizing effect on fluid motion. All these studies emphasize the great significance of external magnetic fields in a filled cavity.

Modern advances in nanotechnology have introduced nanofluids, which are fluids embedded with nanoparticles, as a way to improve thermal performance. Nanofluids do have far better thermal properties and seem to offer very promising potential for improving the heat transfer rates in convective processes. Combining the base fluid with nanoparticles raises its thermal conductivity; such changes can change the dynamics of convection considerably and raise the overall efficiency of the system. Most researchers agree that when nanoparticles are dispersed into a base fluid, the thermal performance of the nanofluid is improved. Other scientists claim that the dispersion could decrease heat transfer to a great extent. The impact of nanofluids on heat transfer could be dependent on the models adopted for the thermal properties of the nanofluids, pertinent parameters, and simplifying hypotheses [10]. Nemati et al. [11] studied the combined effect of CuO nanoparticles and a magnetic field on the Nusselt number in rectangular cavities and found that in the presence of a high magnetic field, the effect of nanoparticles decreases. Ighris et al. [12] showed that the optimal thermal performance can be achieved by optimizing the heater configuration in terms of position, dimension, and orientation.

Despite the significant scientific literature published on natural convection, magnetohydrodynamic flow, as well as heat transfer in nanofluids, the influence of the combination of these phenomena in rectangular enclosures remains not well understood, especially in the case where thermal flux boundary conditions are imposed. On the other hand, the novelty in the present work consists in the analysis of the impact of the combination of the Hartmann number, the aspect ratio of the cavity, as well as the nanoparticle volume fraction on the flow and heat transfer in rectangular enclosures filled with water-Al_2O_3 nanofluids. Moreover, the influence of the cavity geometry as well as the orientation in the aforementioned phenomena is explicitly addressed in the present work. It is in these regards that we try to open up new insights into these interactions to come up with more efficient thermal management solutions across different industrial technologies.

2 Mathematical formulation

2.1 Problem description

A rectangular cavity of width, *W*, and height, *H*, contains a mixture of Al_2O_3 (alumina) nano-solids suspended in water. The horizontal boundaries are insulated, while the vertical ones are under the influence of heat fluxes *q*. The cavity is subjected to a horizontal external magnetic field *B*, see Fig. 1. It has to be emphasized that most studies, for simplicity reasons, assumed Dirichlet boundary conditions, while the majority of the real applications involved Neumann conditions as adopted in this study. The latter thermal condition imposes a non-uniformity of the temperature on the vertical walls, which is more realistic.

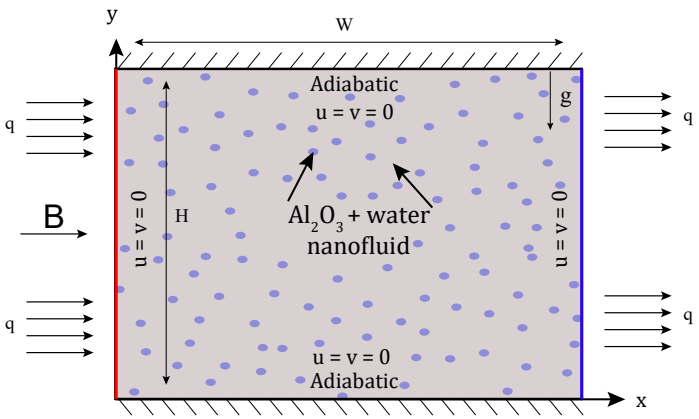

Fig. 1. Enclosure under magnetic field.

The mixture acts as an incompressible, single-phase, and Newtonian nanofluid. The base fluid and nanoparticles are in thermal equilibrium, and the flow is laminar. Table 1 presents the thermophysical properties of the base fluid and nanoparticles. Moreover, the nanofluid density obeys the Boussinesq model in the buoyancy force, while the induced magnetic field, dissipation, and Joule heating are not taken into account.

Table 1. Properties of water and the used nanoparticles.

	ρ(kg m^{-3})	β(K^{-1})×10^5	c_p(J K^{-1}kg^{-1})	k(W K^{-1}m^{-1})	σ(Ω m^{-1})
Al_2O_3	3970.0	0.85	765.0	40.0	0.05

H_2O	997.1	21.0	4179.0	0.613	1×10^{-10}

2.2 Governing equations

The equations of conservation of mass (1), momentum (2) and (3), and energy (4), along with the associated boundary conditions (5 and 6), given the previously listed assumptions, can be written as:

$$\frac{\partial u'}{\partial x'}+\frac{\partial v'}{\partial y'}=0 \quad (1)$$

$$u'\frac{\partial u'}{\partial x'}+v'\frac{\partial u'}{\partial y'}=-\frac{1}{\rho_n}\frac{\partial P'}{\partial x'}+\frac{1}{\rho_n}\left(\frac{\partial}{\partial x'}\left(2\mu_n'\frac{\partial u'}{\partial x'}\right)+\frac{\partial}{\partial y'}\left(\mu_n'\left(\frac{\partial u'}{\partial y'}+\frac{\partial v'}{\partial x'}\right)\right)\right) \quad (2)$$

$$u'\frac{\partial v'}{\partial x'}+v'\frac{\partial v'}{\partial y'}=-\frac{1}{\rho_n}\frac{\partial P'}{\partial y'}+\frac{1}{\rho_n}\left(\frac{\partial}{\partial y'}\left(2\mu_n'\frac{\partial v'}{\partial y'}\right)+\frac{\partial}{\partial x'}\left(\mu_n'\left(\frac{\partial u'}{\partial y'}+\frac{\partial v'}{\partial x'}\right)\right)\right)+g\beta_{Tn}(T'-T'_0)-\frac{\sigma_n}{\rho_n}B^2v' \quad (3)$$

$$u'\frac{\partial T'}{\partial x'}+v'\frac{\partial T'}{\partial y'}=\alpha_n\left(\frac{\partial^2T'}{\partial x'^2}+\frac{\partial^2T'}{\partial y'^2}\right) \quad (4)$$

$$\text{for } y'=0\,,H:\ u'=v'=0 \text{ and } \frac{\partial T'}{\partial y'}=0 \quad (5)$$

$$\text{for } x'=0\,,W:\ u'=v'=0 \text{ and } -k_n\frac{\partial T'}{\partial x'}=q \quad (6)$$

To aid in the analysis and allow numerical simulation, the above-mentioned governing equations (1-6) are transformed into dimensionless equations through dimensional analysis. The following scales with respect to the thermophysical properties water are employed within this analysis:

$$(x,y)=\frac{(x',y')}{H}\,;P=\frac{H^2P'}{\rho_w\alpha_w^2}\,;\ T=\frac{(T'-T_0')}{\Delta T}\,;(u,v)=\frac{H}{\alpha_w}(u',v')\,;\Delta T=\frac{q'H}{k_w} \quad (7)$$

The dimensionless equations describing the problem in the vorticity formulation with the dimensionless boundary conditions are:

$$-\Omega=\nabla^2\Psi \quad (8)$$

$$u\frac{\partial\Omega}{\partial x}+v\frac{\partial\Omega}{\partial y}=\nu_rPr\nabla^2\Omega+\beta_rPrRa\frac{\partial T}{\partial x}-\frac{\sigma_r}{\rho_r}PrHa^2\frac{\partial v}{\partial x} \quad (9)$$

$$u\frac{\partial T}{\partial x}+v\frac{\partial T}{\partial y}=\alpha_r\left(\frac{\partial^2T}{\partial x^2}+\frac{\partial^2T}{\partial y^2}\right) \quad (10)$$

$$\frac{\partial T}{\partial y}=0\,;\ u=v=\Psi=0\,;\ \text{for } y=0,1 \quad (11)$$

$$\frac{\partial T}{\partial x}+\frac{1}{kr}=0\,;\ u=v=\Psi=0\,;\ \text{for } x=0,A \quad (12)$$

The dimensionless governing parameters are the Prandtl, Rayleigh, and Hartmann numbers and the aspect ratio of the enclosure.

$$Pr=\frac{\nu_w}{\alpha_w};Ra=\frac{g\beta_{Tw}H^3\Delta T}{\nu_w\alpha_w};Ha=BH\sqrt{\frac{\sigma_w}{\nu_w\rho_w}};A=\frac{W}{H} \quad (13)$$

The dynamic viscosity and thermal conductivity of the Al_2O_3-water nanofluid are estimated by the experimental models of Maiga, and other properties are modeled as in [10].

These models are valid for a concentration below 5% to ensure the suspension of the nanoparticles in the base fluid.

$$\mu_r = 123\varphi^2 + 7.3\varphi + 1 \quad (14)$$
$$k_r = 4.97\varphi^2 + 2.72\varphi + 1 \quad (15)$$

The dimensionless quantity for the average rate of heat transfer, as well as the enhancement ratio, which compares the heat transfer in the nanofluid to that of water, is given by:

$$\overline{Nu} = \int_0^1 \frac{A}{T(0,y)-T(A,y)}\,dy \;;\; \overline{Nu}_r(\%) = \frac{\overline{Nu}(\varphi)-\overline{Nu}(\varphi=0)}{\overline{Nu}(\varphi=0)} \times 100 \quad (16)$$

3 Numerical method

To address the problem in this study, an in-house FORTRAN code using the finite difference method is employed. The first and second-order spatial partial derivatives, mentioned in the basic equations, are discretized using a central finite difference formulation. For the solution of the set of equations (9-12) [13], the Alternating Implicit Direction (ADI) technique is chosen to be utilized in this study, so the system of partial differential equations describing the problem is replaced by a system of algebraic equations. Additionally, the point Successive Over-Relaxation (PSOR) method is chosen to be employed to solve the continuity equation (8). The calculation of the solution is terminated when the absolute convergence criterion of $\sum\sum\left|f_{i,j}^{k+1} - f_{i,j}^{k}\right| \leq 10^{-12}\sum\sum\left|f_{i,j}^{k+1}\right|$, was achieved.

3.1 Validation of the code

The results obtained from the present numerical solution are compared with those of previous research studies [14, 15] to check the accuracy, as can be seen from Tables 2 and 3. These tables compare the results of the present code in terms of $\overline{Nu}$ and Ψ_{max} with an experimental study of Ho et al. [15] for nanofluids under natural convection and a numerical one under a magnetic field conducted by Ghasemi et al. [14]. As listed in these tables, it is clear that the present code exhibits a perfect agreement with those studies, with a maximal relative difference of 1.5%. Thus, we are confident in our elaborated numerical code to solve the problem at hand.

Table 2. Comparison with the experimental *Nu* of nanofluid natural convection for different φ.

φ	1%	2%	3%
Experimental data [15]	32.20	31.09	29.07
Present study	32.25	30.94	29.46
Relative difference (%)	0.16	0.48	1.34

Table 3. Comparison with the numerical $|\Psi_{\max}|$ and $\overline{\mathrm{Nu}}$ of the nanofluid under a magnetic field.

	Ha	0	30	60
Ghasemi et al. [14]	$\overline{Nu}$	4.96	3.10	1.80
	$\lvert\Psi_{max}\rvert$	11.80	5.59	2.31
Present study	$\overline{Nu}$	4.96	3.11	1.80
	$\lvert\Psi_{max}\rvert$	11.77	5.58	2.31
Relative difference (%)	$\overline{Nu}$	0.00	0.32	0.00
	$\lvert\Psi_{max}\rvert$	0.25	0.18	0.00

3.2 Mesh independence

The numerical simulations were performed using several uniform grids to determine the sensitivity to the discretization of the solution in space and to determine the grid-independent solutions. Regarding the cavity aspect ratio, it is indicated in Table 4 that the values for the average Nusselt number and the maximum stream function remain unaltered for the increased refinement up to the 101 × 101 grid. Further refinement beyond this grid size shows that the changes are marginal, 0.24% and 0.06% of the relative variation against the 181 × 181 grid size in terms of the average Nusselt number and the maximum stream function, respectively. The results indicate that the thermal and velocity boundary layers are already captured accurately.

Table 4. Mesh effect on $\lvert\Psi_{max}\rvert$ and $\overline{Nu}$ of the nanofluid under a magnetic field in a horizontal cavity with the relative variation against the finest mesh.

	41	61	101	141	181
$\overline{Nu}$	2.962 (2.52%)	2.925 (1.24%)	2.896 (0.24%)	2.893(0.13%)	2.889
$\lvert\Psi_{max}\rvert$	3.096 (0.35%)	3.097 (0.32%)	3.105 (0.06%)	3.106 (0.03%)	3.107

4 Results and discussion

The numerical results of this work are presented in terms of the average Nusselt number and flow intensity in the centre of the cavity, and also the enhancement ratio for values of $0 \leq \varphi \leq 0.05$, $0.25 \leq A \leq 4$, and $0 \leq Ha \leq 80$. In this study, we chose $Pr = 6.5$ to represent water as the base fluid and $Ra = 10^4$ because, according to our previous study, at this value, the change of the nanofluid behaviour can be captured compared to $Ra = 10^5$, where it shows only a deterioration [10].

Figure 2 illustrates the coupled dynamical and thermal structures of the flow through streamlines and isotherms for an aspect ratio $A = 2$, comparing the non-magnetic case ($Ha = 0$) and a strong magnetic field ($Ha = 80$), in the absence ($\varphi = 0$, black lines) and presence (φ

= 0.05, red lines) of nanoparticles. For the case where *Ha* = 0, the buoyancy forces are significant, and a well-developed convective circulation with strong primary vortices is present. The velocity field demonstrates a high level of fluid circulation, which enhances the thermal mixing within the cavity. Accordingly, the isotherms are highly distorted from the vertical. Adding the nanoparticles results in a slightly less intense circulation due to the changes in the effective viscosity, and the thermal stratification near the hot and cold surfaces remains less distorted. Finally, the application of the magnetic field results in a significant reduction in the flow velocity. At *Ha* = 80, an important decrease in the circulation velocity was observed for the two nanoparticle concentrations. The magnetic field has a significant effect on the flow field, as the Lorentz forces are significant and act against the fluid motion. Accordingly, the circulation velocity is greatly reduced. The isotherms are less inclined. The effect of the magnetic field is larger in the nanofluid case. Accordingly, the isotherms are less inclined and are confined near the cavity walls. A comparison of the results obtained with φ = 0 and 0.05 at high values of the Hartmann number demonstrates that the addition of the nanoparticles results in a tighter distribution of the isotherms near the hot surface.

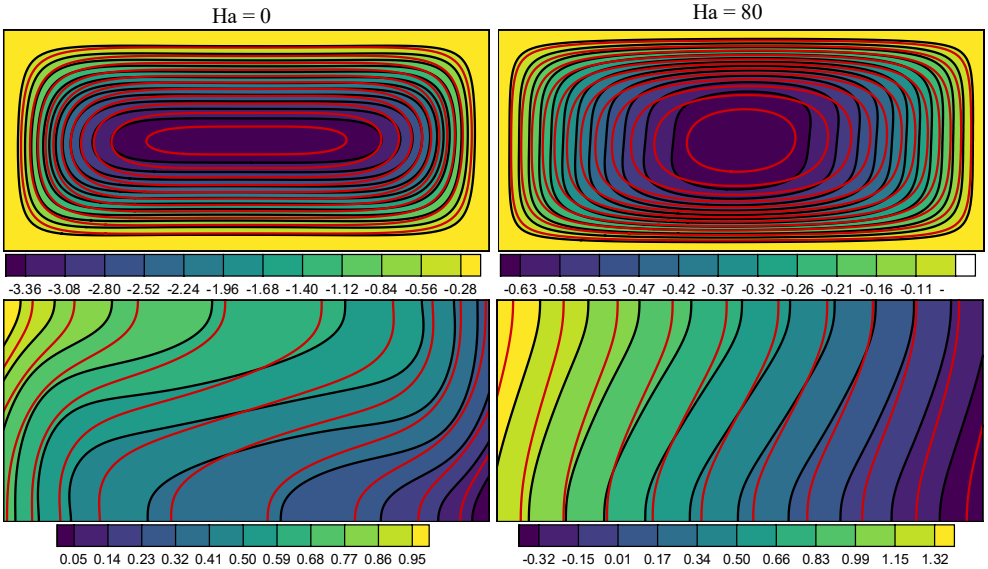

Fig. 2. Streamlines and isotherms for different φ and *Ha*.

The effect of the geometrical parameter *A* on the flow intensity and heat transfer rate inside the cavity is depicted in Fig. 3(a and b) for selected *Ha* and φ. The flow intensity is an increasing function with the increase in *A* for all the values of *Ha* and φ (Fig. 3a). Physically, the increase in the geometric value of *A* expands the area of the fluid and thus the development of the buoyancy-driven circulation. The nanofluid rotating in a clockwise direction has more space to accelerate, enhance the thermal boundary layers, and establish a stronger convective cell. However, as the value of *A* continues to increase, the amplitude of the resulting stream function, Ψ_c, eventually attains an asymptotic value due to the full development of the buoyancy-driven circulation, and thus the additional space will no longer enhance the mixing efficiency. The presence of the magnetic field retards this process of saturation. Due to the presence of the externally applied magnetic field and the interaction of the electrically conducting nanofluid, the generated force increases with the magnetic field strength and resists the fluid flow. The magnetic effects dampen the velocity gradients and make the flow more stable and less capable of attaining the full development of the circulation cell due to buoyancy forces. The independence of the asymptotic value of Ψ_c from the

geometric parameter A is delayed for higher values of A, implying that the expansion of geometry is needed to attain the natural saturation point of the flow process under a magnetic field.

The effect of nanoparticles on the flow intensity is negative, since the presence of solid particles contributes to the enhancement of effective viscosity in the suspension. The strengthened viscous boundary reduces the rate of internal convection and therefore exerts a lesser effect on the value of Ψ_c. However, this negative effect is reduced by the presence of a magnetic field. The magnetic convection reduces the effect of flow intensity because the magnetic damping has already caused a decline in flow intensity due to the presence of nanofluids. The effect exerted by the presence of the magnetic convection is to make the nanoparticles less effective in exerting their suppression effect on the flow intensity due to the presence of a higher viscosity. This means that the negative effect of nanofluid viscosity can be adjusted by applying a magnetic field.

The variation of the rate of heat transfer with A indicates a monotonic increase and can clearly be ascribed to the accompanying increase in the intensity of flow (Fig. 3b). With an increase in A, the region available for buoyancy-induced convective motion expands, and hence the stirring of the fluid intensifies, leading to a decrease in the thermal boundary layer on the heated surface and enhancing the effective transport of heat to cold regions. On the other hand, the dependence of $\overline{Nu}$ and the nanoparticle volume fraction φ displays a non-monotonic, or double, behaviour that depends significantly on A and Ha. Without the presence of the magnetic field, the addition of nanoparticles, for smaller cavities ($A < 0.5$), results in the enhancement of $\overline{Nu}$. In that regime, although the convective flow becomes moderately developed, the contribution from the increase in the effective thermal conductivity by the addition of the nanoparticles becomes the predominant effect. The strengthened advective heat transport through the fluid mitigates the corresponding rise in the viscosity, causing $\overline{Nu}$ to increase. For $A > 0.5$, due to the sufficiently developed convection, viscous forces become more prominent. The effect of the elevated viscosity, corresponding to the enhancement of the nanoparticle loading, reduces the buoyancy-driven flow, diminishing the intensity of the circulation, and the boundary layers become thicker. In that case, the detrimental effect caused by the increase in viscosity overpowers the contribution from the increase in the effective heat transport through the enhanced thermal conductivity, and the heat transfer rate deteriorates. This happens especially for an aspect ratio higher than the critical value $A_{cr,}$ where the effect of the nanoparticle on heat transfer changes from enhancement to deterioration.

The presence of a magnetic field ($Ha = 30$) triggers the additional damping effect caused by the Lorentz force, completely changing the balance because of the following reasons: The presence of the magnetic field dampens the velocity fluctuations and hence hinders the buoyancy effects and suppresses the contribution of convection to the heat transfer rate. Therefore, a nanoparticle-induced viscosity effect will have less significance for a larger value of A, because the flow is already resisted by the magnetic effect. This implies that the geometrical parameter at which the changeover, or transition, from enhancement to deterioration occurs at a significantly larger critical value ($A_{cr} \approx 2.7$). This implies that the effect of nanoparticles can be sustained even for an elongated enclosure when the buoyancy effect is sufficient to resist the magnetic damping effect. Therefore, a combination of geometries and the presence of a magnetic field offers a viable option to enhance the heat transfer rate by employing nanofluids for a variety of configurations.

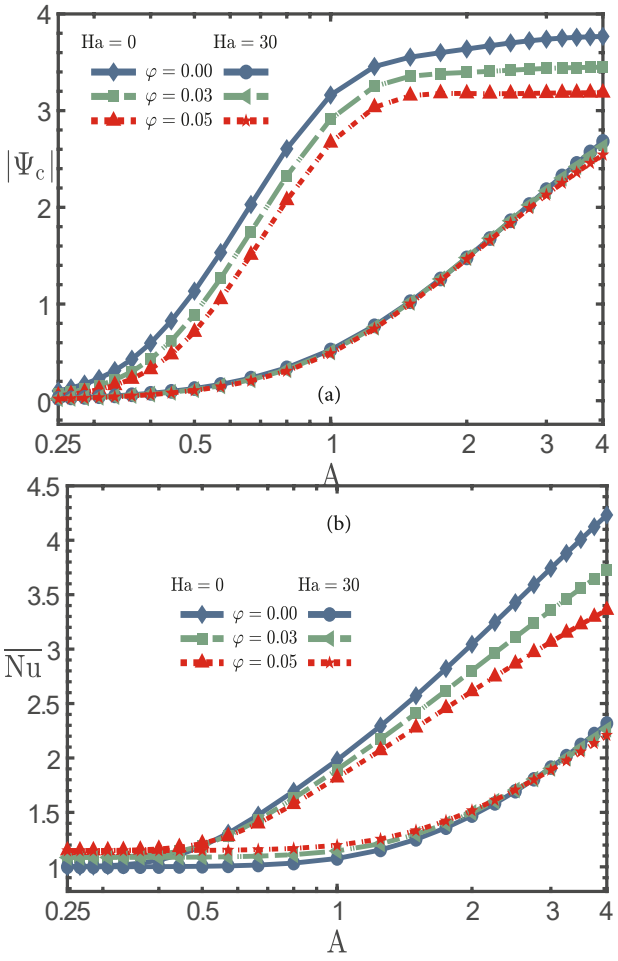

Fig. 3. Variations of $\overline{Nu}$ and Ψ_c vs A for different φ and Ha.

The impact of magnetic field intensity on $\overline{Nu}$ is shown in Fig. 4a. From this figure, it can be found that with an increase in Ha, the average Nusselt number tends to decrease. This occurred because of the presence of the Lorentz force in this phenomenon, which acts as an opposing force. Although this is an overall damping phenomenon, the presence of nanoparticles can produce a favorable impact on the magnetic field. For the case of vertical cavities, the impact of Ha is found to be insignificant since the process of heat transfer is dominated by conduction and not convection. In this case, the flow is already low because of the geometry of the cavity. The impact of the nanofluid's effective conductivity is significant compared to the impact of the increased viscosity. The application of the nanofluid is thus more favorable compared to the application of water alone, irrespective of the Ha values.

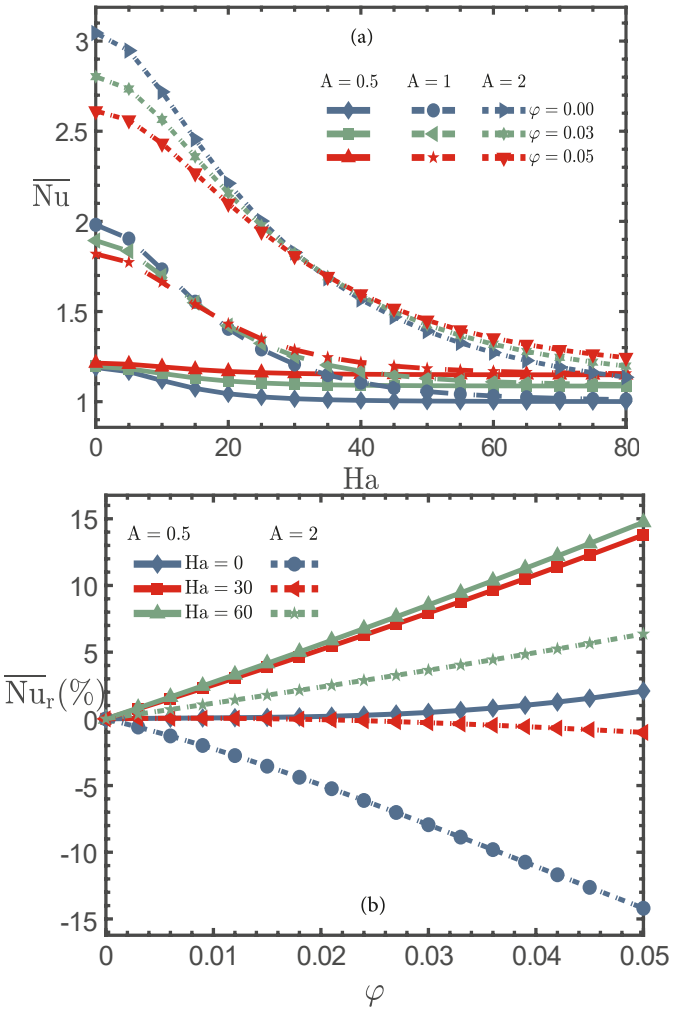

Fig. 4. Variations of $\overline{Nu}$ with *Ha* and the enhancement ratio with φ for various aspect ratios.

However, in square and horizontal cavities, where convective effects are dominated by natural convection, adding nanoparticles initially degrades convective heat transfer in the absence of a magnetic field (*Ha* = 0). The increasing effective viscosity due to nanoparticles mainly contributes to this degradation by reducing buoyancy-driven flows and thickening thermal boundary layers. However, with an increasing magnetic field strength, the resulting Lorentz force gradually diminishes convective dominance effects. For a critical value of *Ha*, there could be sufficient damping of convective effects such that the enhanced thermal conductivity of the nanofluid overpowers the effects of increased viscosity. It is also clear that, for example, in cavities with *A* = 1 and 2, magnetic field strengths above *Ha* = 17 and *Ha* = 32, respectively, are required in order to overcome degradation and start improving convective heat exchange.

In order to quantify this phenomenon further, the plot of the enhancement ratio, $\overline{Nu}_r(\%)$, is shown as a function of φ, for different values of *A* and *Ha*, as depicted in Fig. 4b. For vertical cavity cases, it is evident that the enhancement ratio increases monotonically with *Ha* as well as φ, reaching as high as 15% at *Ha* = 60 and φ = 5%. This variation is consistent with the fact that, under pure conduction conditions, the role of conductivity is more

dominant than that of viscosity. As expected, without the magnetic field, the role of viscosity is dominant, resulting in a negative deterioration of approximately -15%. For a strong magnetic field, $Ha = 60$, the magnetic field dampening term is strong enough to counteract the unwanted role of viscosity, resulting in a net enhancement of about 6%.

5 Conclusions

In summary, the main parameters varied in this work are the geometrical parameter A, magnetic field intensity Ha, and Al_2O_3 volume fraction φ. Results show that the heat transfer rate increases with A due to improved fluid mixing. The Nusselt number versus φ relationship is different depending on A and Ha. In the absence of a magnetic field, there exists some critical value of A beyond which this relationship changes; in the presence of a magnetic field, better nanofluid heat transfer is found to take place for higher A. The enhancement ratio indicates that heat transfer can be increased up to 15% in vertical cavities. For the case at $Ha = 0$, the negative effect of viscosity decreased heat transfer by -15%, which turned to a 6% enhancement at $Ha = 60$. These results show that with proper geometry and magnetic field intensity, one can obtain a significant enhancement in heat transfer within nanofluid-filled cavities.

References

1. Wang, X., Bhowmick, S., Tian, Z.F., Saha, S.C., Xu, F.: Experimental study of natural convection in a V-shape-section cavity. Physics of Fluids. 33, (2021). https://doi.org/10.1063/5.0031104.
2. Chen, H.-T., Hsu, M.-H., Huang, Y.-C., Chang, K.-H.: Experimental and numerical study of inverse natural convection-conduction heat transfer in a cavity with a fin. Numeri. Heat Transf. A Appl. 84, 641–658 (2023). https://doi.org/10.1080/10407782.2022.2153771.
3. Weppe, A., Moreau, F., Saury, D.: Experimental investigation of a turbulent natural convection flow in a cubic cavity with an inner obstacle partially heated. Int. J. Heat Mass Transf. 194, 123052 (2022). https://doi.org/10.1016/j.ijheatmasstransfer.2022.123052.
4. Yoladi, M., Akyurek, E.F., Afshari, F.: Experimental study on the influence of inclination angle on phase change materials and natural convection during melting. J. Energy Storage. 83, 110769 (2024). https://doi.org/10.1016/j.est.2024.110769.
5. Abdulkadhim, A., Abed, I. mejbel, Said, N. mahjoub: An exhaustive review on natural convection within complex enclosures: Influence of various parameters. Chinese Journal of Physics. 74, 365–388 (2021). https://doi.org/10.1016/j.cjph.2021.10.012.
6. Hamid, M., Usman, M., Khan, W.A., Haq, R.U., Tian, Z.: Natural convection and multidirectional magnetic field inside a square shaped cavity with sinusoidal temperature and heated/cold blocks. International Communications in Heat and Mass Transfer. 152, 107291 (2024). https://doi.org/10.1016/j.icheatmasstransfer.2024.107291.
7. Liao, C.C., Li, W.K.: Assessment of the magnetic field influence on heat transfer transition of natural convection within a square cavity. Case Studies in Thermal Engineering. 28, 101638 (2021). https://doi.org/10.1016/J.CSITE.2021.101638.
8. Mohammadi, M., Nassab, S.A.G.: Combined influences of radiation and inclined magnetic field on natural convection in a cavity with complex geometry.

International Communications in Heat and Mass Transfer. 134, 106030 (2022). https://doi.org/10.1016/J.ICHEATMASSTRANSFER.2022.106030.

9. Li, P.-X., Luo, X.-H., Chen, L., Song, J.-J., Li, B.-W., Karcher, C.: Numerical research for the effect of magnetic field on convective transport process of molten salt in Rayleigh-Bénard system. International Journal of Thermal Sciences. 195, 108605 (2024). https://doi.org/10.1016/j.ijthermalsci.2023.108605.
10. El hadoui, B., Tizakast, Y., Tizakast, S., Kaddiri, M.: Modeling and optimization of heat transfer and flow dynamics of non-Newtonian Carreau nanofluids in differentially heated enclosed domains: coupled effects of rheology, geometry, and external forces. Int. J. Heat Fluid Flow. 117, 110110 (2026). https://doi.org/10.1016/J.IJHEATFLUIDFLOW.2025.110110.
11. Nemati, H., Farhadi, M., Sedighi, K., Ashorynejad, H.R., Fattahi, E.: Magnetic field effects on natural convection flow of nanofluid in a rectangular cavity using the Lattice Boltzmann model. Scientia Iranica. 19, 303–310 (2012). https://doi.org/10.1016/j.scient.2012.02.016.
12. Ighris, Y., El hadoui, B., Baliti, J., Elguennouni, Y., Hssikou, M.: Optimizing thermal management of convective heat transfer in a complex nanofluid-filled cavity using the lattice Boltzmann method. Int. J. Numer. Methods Heat Fluid Flow. (2025). https://doi.org/10.1108/HFF-01-2025-0044.
13. El hadoui, B., Kaddiri, M.: Comparing Two Numerical Methods in the Case of Aiding and Opposing Natural Double Diffusion in a Square Enclosure. In: 2024 4th International Conference on Innovative Research in Applied Science, Engineering and Technology (IRASET). pp. 1–5. IEEE (2024). https://doi.org/10.1109/IRASET60544.2024.10548769.
14. Ghasemi, B., Aminossadati, S.M., Raisi, A.: Magnetic field effect on natural convection in a nanofluid-filled square enclosure. International Journal of Thermal Sciences. 50, 1748–1756 (2011). https://doi.org/10.1016/j.ijthermalsci.2011.04.010.
15. Ho, C.J., Liu, W.K., Chang, Y.S., Lin, C.C.: Natural convection heat transfer of alumina-water nanofluid in vertical square enclosures: An experimental study. International Journal of Thermal Sciences. 49, 1345–1353 (2010). https://doi.org/10.1016/j.ijthermalsci.2010.02.013.